Available online at www.sciencedirect.com
SCIENCE DIRECT®
Journal of Solid State Chemistry 176 (2003) 120–126
JOURNAL OF SOLID STATE CHEMISTRY
http://elsevier.com/locate/jssc

Molecular motion in solid ammonia trimethylalane

Gianina Tutoveanu,[a] Simon J. Kitchin,[a] Kenneth D.M. Harris,[a,*] and Jens Müller[b,c]

[a] *School of Chemical Sciences, University of Birmingham, Edgbaston, Birmingham B15 2TT, UK*
[b] *Faculty of Chemistry, University of Bochum, D-44780 Bochum, Germany*
[c] *Department of Chemistry, University of Saskatchewan, 110 Science Place, Sask., Canada SK S7N 5C9*

Received 26 March 2003; received in revised form 16 June 2003; accepted 28 June 2003

Abstract

Solid state ^{2}H NMR has been used to study molecular motion in deuterated ammonia trimethylalane $(CH_3)_3AlND_3$. From analysis of the ^{2}H NMR lineshape between 123 and 298 K, reorientation of the $-ND_3$ group about the molecular Al–N axis is shown to occur at a rate higher than $10^8\,s^{-1}$, and simulation of partially relaxed ^{2}H NMR lineshapes shows that the reorientation can be described as a 3-site 120° jump motion. From the temperature dependence of the ^{2}H spin–lattice relaxation time, the activation energy for this motion is estimated to be $9.3 \pm 0.3\,kJ\,mol^{-1}$. There is no evidence from either ^{2}H or ^{27}Al NMR data for any site-exchange between the sites occupied by the $-ND_3$ and $-CH_3$ groups. The anisotropy of the dynamics of $(CH_3)_3AlND_3$ indicates that the orientation of the Al–N bond is highly constrained, presumably by a strong interaction between the electric dipoles of neighboring molecules.

1. Introduction

Molecules in crystalline solids can undergo substantial reorientational motions, typified by "rotator phase" solids (plastic crystals) [1,2]. Molecules that are essentially cylindrical in shape (e.g., *n*-alkanes [3–6]) or essentially spherical in shape (e.g., buckminsterfullerene (C_{60}) [7–9]) often exhibit a rotator phase at sufficiently high temperature, in which the individual molecules reorient rapidly within the solid. In the former case, rapid reorientation occurs about a single axis (the cylinder axis), whereas in the latter case, the reorientation is essentially isotropic or at least involves pseudo-isotropic averaging. Other molecules such as adamantane [10,11], neopentane [12–14], tetramethylsilane [15,16], tetrakis(trimethylsilyl)silane [17,18] and tetrakis(trimethylsilyl)methane [19] are also found to exhibit rotator phases in the solid state. Although the molecular symmetry in each of these cases is tetrahedral, the molecular shapes are actually rather globular (i.e., approximating to spherical), and it is not surprising on steric grounds that substantial reorientation (in the form of tetrahedral jump motions or essentially isotropic reorientations) can occur within the volume of space occupied by these molecules in their crystal structures.

In the present paper, we explore the dynamic properties of ammonia trimethylalane $(CH_3)_3AlNH_3$ (Fig. 1; abbreviated ATMA). This molecule is isoelectronic with tetramethylsilane $[(CH_3)_3SiCH_3]$, and geometrically the ATMA molecule may be described as pseudo-tetrahedral X_3MX' (the true molecular symmetry is actually lower than tetrahedral, with a three-fold axis along the Al–N bond). Thus, on steric considerations, it might be anticipated that ATMA could exhibit a rotator phase in which the $-NH_3$ and $-CH_3$ groups exchange sites, similar to the type of motion observed for tetramethylsilane and other rotator phase solids based on tetrahedral molecules discussed above. Nevertheless, depending on the actual environment of the molecule in the crystal structure and the nature of the local intermolecular interactions (which may be significantly different for the $-NH_3$ and $-CH_3$ groups), the reorientational freedom of the molecule may be significantly more constrained. The crystal structure of ATMA, established from powder X-ray diffraction data, has been reported previously [20]. The reported structure implies that the locations of the $-NH_3$ and $-CH_3$ groups are ordered, corresponding to linear arrays of molecules with their Al–N bonds parallel, although it is pertinent

*Corresponding author. Fax: +44-121-414-7473.
E-mail address: k.d.m.harris@bham.ac.uk (K.D.M. Harris).

0022-4596/$ - see front matter © 2003 Elsevier Inc. All rights reserved.
doi:10.1016/S0022-4596(03)00355-4

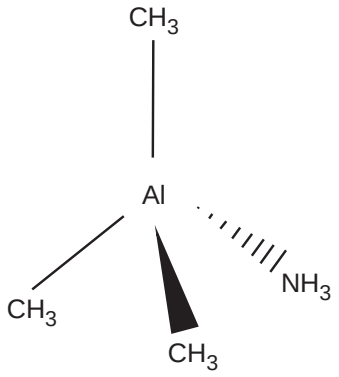

Fig. 1. Molecular structure of ammonia trimethylalane $(CH_3)_3AlNH_3$.

to question the ability of powder X-ray diffraction to unambiguously distinguish the $–NH_3$ and $–CH_3$ groups, given their very similar X-ray scattering powers. The present work to investigate the dynamic properties of ATMA therefore provides an opportunity to assess independently the issue of order versus (dynamic) disorder of the $–NH_3$ and $–CH_3$ groups in this structure.

Our investigation of the dynamic properties of ATMA has focused on ^{2}H NMR lineshape analysis and ^{2}H NMR spin–lattice relaxation time measurements for N-deuterated ATMA [i.e., $(CH_3)_3AlND_3$; abbreviated ATMA-d_3], together with ^{27}Al NMR lineshape analysis. ^{2}H NMR spectroscopy is a particularly powerful technique for studying molecular reorientation in solids [21–28], and has been applied to study a wide variety of types of dynamic process in a broad range of materials. When the rate of motion is in the range 10^3–10^8 s^{-1} (the intermediate motion regime), analysis of the ^{2}H NMR lineshape provides detailed information on the rate and mechanism of the dynamic process. For rates of motion higher than 10^8 s^{-1} (rapid motion regime), the actual rate of motion cannot be established from ^{2}H NMR lineshape analysis, but information on the geometry and mechanism of the motion can nevertheless be obtained. ^{2}H NMR lineshape analysis is generally carried out by calculating the lineshapes for proposed dynamic models, and finding the dynamic model for which the set of calculated lineshapes provides the best fit to the set of experimental lineshapes recorded as a function of temperature. When the rate of motion is in the rapid regime with respect to ^{2}H NMR lineshape analysis, detailed dynamic information can be obtained from measurement and analysis of the ^{2}H NMR spin–lattice relaxation time (T_1), which is particularly sensitive for studying dynamic processes with rates in the range $10^{-3}\nu$ to $10^3\nu$ (where ν is the ^{2}H Larmor frequency). In this paper, we employ both ^{2}H NMR lineshape analysis and ^{2}H NMR spin–lattice relaxation time measurements to investigate the dynamic properties of ATMA-d_3.

We note that solid state ^{1}H NMR techniques may also be used to elucidate dynamic properties of molecular solids, and have been applied previously to study dynamics of other molecular solids of the general type $(CH_3)_3X–YH_3$ ($Y \neq C$), such as $(CH_3)_3N–BH_3$ [29,30], although to our knowledge no such techniques have been applied to investigate dynamic properties of ATMA.

2. Experimental

2.1. Sample preparation and handling

ATMA-d_3 was prepared and purified according to standard literature methods [31]. The sample was cold sealed in a glass ampoule for use in the solid state NMR experiments. All handling of the sample was carried out at or below ambient temperature, as it is known that decomposition of ATMA occurs at ca. 50–60°C. In order to avoid sample decomposition, our studies of the solid state dynamics of ATMA-d_3 (see below) have been carried out at ambient temperature (298 K) and lower temperatures (down to 123 K). Previous differential scanning calorimetry studies [32] suggest that ATMA does not undergo any phase transitions (at which changes in the dynamic behavior might be anticipated) between ambient temperature and the decomposition temperature.

2.2. Solid state ^{2}H NMR

Solid state ^{2}H NMR spectra of ATMA-d_3 were recorded at 46.079 MHz on a Chemagnetics CMX Infinity 300 spectrometer using a non-spinning probe with 5 mm (i.d.) coil. The standard quadrupole echo pulse sequence $[(\pi/2)_\phi - \tau - (\pi/2)_{\phi\pm\pi/2} - \tau' -$acquire$-$recycle] was used, with a $(\pi/2)$ pulse duration of 2 μs and an eight step phase cycle. The delay between pulses (τ) was 30 μs and the recycle delay was longer than five times the estimated value of T_1 at each temperature.

The powder average ^{2}H NMR spin–lattice relaxation time $\langle 1/T_1 \rangle_p^{-1}$ was measured between 133 and 283 K using the saturation-recovery technique. The pulse sequence was $[(\tau_d - (\pi/2)_\varphi)_n - \tau_r - (\pi/2)_\phi - \tau -$ $(\pi/2)_{\phi\pm\pi/2} - \tau' -$acquire$-$recycle], where $n = 30$, $\tau_d = 500$ μs and τ_r (the relaxation delay) was calculated according to $\tau_r = \tau_0\ (10^{1/10})^{N-1}$, where N is the delay number and τ_0 is the duration of the first delay. At each temperature, 42 values of τ_r were used. The saturation-recovery data were fitted using the spectrometer software.

Inversion-recovery spectra were recorded at 298 K using a pulse sequence modified for ^{2}H nuclei [33]. This pulse sequence comprises a composite π pulse followed by the quadrupole echo sequence: $\{[(CP)(\overline{CP})(CP)]_\phi$

$-\tau_r - (\pi/2)_{\phi} - \tau - (\pi/2)_{\phi\pm\pi/2} - \tau' -$acquire–recycle$\}$, where $\tau = 30\,\mu s$ and (CP) $\equiv \overline{17}°, 62°, \overline{99}°, 142°$ (the overbar indicates a 180° phase shift).

2.3. Solid state ^{27}Al NMR

Solid state ^{27}Al NMR spectra were recorded at 78.218 MHz on a Chemagnetics CMX Infinity 300 spectrometer for a non-spinning sample of ATMA-d_3 using a double resonance goniometer probe (7 mm (i.d.) coil). The standard spin echo pulse sequence $[(\pi/2)_{\phi} - \tau - (\pi)_{\phi\pm\pi/2} - \tau' -$acquire$-$recycle] was used with ^{1}H decoupling (decoupler field strength ca. 40 kHz), a $(\pi/2)$ pulse duration of 2 μs and a 16 step phase cycle. The delay (τ) between pulses was 50 μs and the recycle delay was longer than five times the estimated value of T_1 for ^{27}Al.

2.4. Lineshape simulations

In describing dynamic processes by jump models in simulations of ^{2}H NMR lineshapes, each ^{2}H site is specified by the Euler angles $\{\alpha, \beta, \gamma\}$ that define the orientation (relative to a space fixed reference frame) of the principal axis system of the electric field gradient tensor ($\mathbf{V}^{PAS}$) at the ^{2}H nucleus. The components of $\mathbf{V}^{PAS}$ are defined such that $|V_{ZZ}| \geqslant |V_{YY}| \geqslant |V_{XX}|$. The quadrupole coupling constant χ is defined as eQV_{ZZ}/h, where Q is the quadrupole moment of the ^{2}H nucleus, and the asymmetry parameter η is defined as $||V_{YY}|-|V_{XX}||/|V_{ZZ}|$, with $0 \leqslant \eta \leqslant 1$.

Simulations of the ^{2}H NMR lineshapes were carried out using the MXQET program [34], and simulations of inversion-recovery spectra were carried out using a slightly modified version of the MXET1 program [24]. In both cases, the dynamic model for the simulations was based on a 3-site 120° jump motion about an axis collinear with the Al–N bond of ATMA-d_3, with equal populations of the three sites and equal jump rates between the three sites. Each site was taken to have the same values of χ and η, and the z-axis of $\mathbf{V}^{PAS}$ for each site was assumed to be coincident with the N–D bond vector.

Simulations of the ^{27}Al NMR spectra were carried out using a modified version of the CQP program [35]. In these simulations, no dynamic model was used.

3. Results and discussion

3.1. ^2H NMR lineshape analysis

Solid state ^{2}H NMR spectra of ATMA-d_3 recorded in the temperature range 123–298 K are shown in Fig. 2. The lineshape at 298 K consists of a narrow Pake powder pattern, with a splitting $\Delta\nu_s = 50.2$ kHz between the main peaks, and with a motionally averaged asymmetry parameter of zero. The spectrum is consistent with reorientation of the –ND_3 group about the Al–N axis in the rapid motion regime (i.e., at a rate $\kappa \geqslant 10^8\,s^{-1}$). For such motion, it can be shown (assuming $\eta = 0$) that the splitting $\Delta\nu_s$ is given by

$$\Delta\nu_s = \frac{3\chi}{4}|(3\cos^2\beta - 1)/2|, \quad (1)$$

where β is the angle between the N–D bond and the Al–N axis (the rotation axis). Taking $\beta = 70.5°$ (calculated on the basis of tetrahedral geometry) and $\Delta\nu_s = 50.2$ kHz, Eq. (1) gives a static quadrupole coupling constant $\chi \approx 201$ kHz. On decreasing temperature to 123 K, the ^{2}H NMR lineshape remains virtually unchanged, indicating that the rate of reorientation of the ND_3 group is in the rapid motion regime at all temperatures down to 123 K.

A narrow central peak is present in the spectra recorded between 198 and 298 K (Fig. 2) and may arise from a very low population of ATMA-d_3 molecules for which there is either rapid isotropic motion (e.g., in the gas phase), or fast exchange between the –ND_3 and –CH_3 groups in a tetrahedral jump motion (e.g., at the surface of the material and/or in the vicinity of defect sites). Although a possible reason for this narrow central

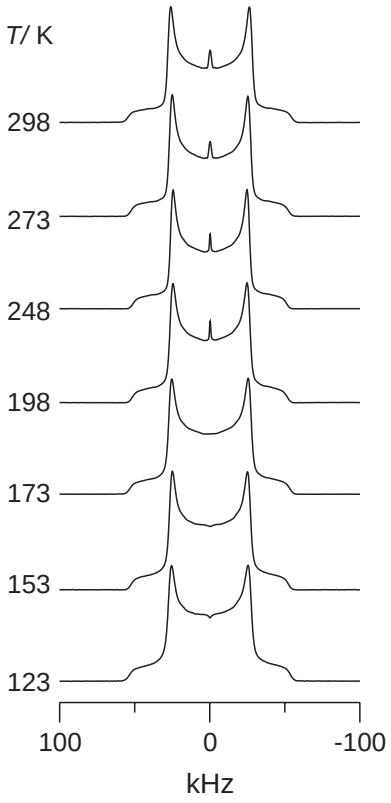

Fig. 2. Experimental ^{2}H NMR spectra recorded for ATMA-d_3 as a function of temperature using the quadrupole-echo pulse sequence with $\tau = 30\,\mu s$.

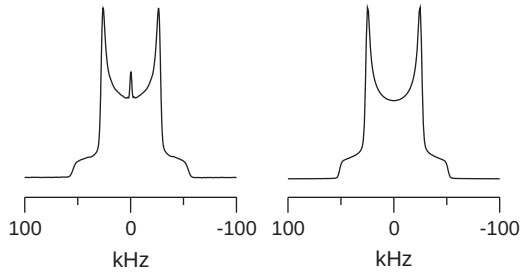

Fig. 3. Left—experimental ^{2}H NMR spectrum of ATMA-d_3 recorded at 298 K with $\tau = 30\,\mu s$. Right—simulated ^{2}H NMR spectrum calculated using the 3-site 120° jump model discussed in the text.

peak could be partial decomposition of the sample to give ammonia (ND_3), we do not believe that significant decomposition could occur under the conditions of sample handling in our work (see Section 2.1). At 123 K, there is a small dip in the center of the spectrum. As shown recently [36], this type of feature may occur when the dominant dynamic process is in the extreme narrowing regime (i.e., $\tau_c \ll \omega_0^{-1}$, where τ_c is the correlation time for the motion). At higher temperatures, this feature is presumably obscured by the central peak.

The ^{2}H NMR spectra were simulated successfully using the 3-site 120° jump motion described in Section 2.4, with $\beta = 70.5°$ and static asymmetry parameter $\eta = 0$ for each site. No attempt was made to fit the central line or the dip in the center of the spectrum. The experimental spectrum recorded at 298 K and the best-fit simulation of this spectrum are shown in Fig. 3. The jump rate κ [note: $\kappa = 1/(3\tau_c)$] for this simulation, and for the best-fit simulations at all temperatures from 298 to 123 K, is in the rapid motion regime ($\kappa \geqslant 10^8\,s^{-1}$), in which the lineshape is independent of the actual value of κ. The good agreement between simulated and experimental lineshapes at all temperatures confirms that the only large amplitude motion of the $-ND_3$ group that occurs on the timescale probed by ^{2}H NMR lineshape analysis (i.e., occurring at a rate of ca. $10^3\,s^{-1}$ or higher) is rapid reorientation (via 120° jumps) about the Al–N axis. From the best-fit ^{2}H NMR lineshape simulation at each temperature, the fitted value of the static quadrupole coupling constant (χ) decreases slightly on increasing temperature (207 kHz at 123 K; 204 kHz at 298 K). This slight reduction in χ as temperature is increased subsumes the effects of an increase in the amplitude of any rapid, small-amplitude motions (e.g., librational motions) that may occur in this temperature range.

3.2. ^{2}H NMR spin–lattice relaxation

Powder average ^{2}H NMR spin–lattice relaxation times $\langle 1/T_1 \rangle_p^{-1}$ were measured in the temperature range 133–283 K and a plot of $\ln(\langle 1/T_1 \rangle_p^{-1}/s)$ versus $(T/K)^{-1}$ is shown in Fig. 4. It is clear that $\langle 1/T_1 \rangle_p^{-1}$ decreases (approximately linearly) as temperature is increased, indicating that the motional process dominating the relaxation is in the extreme-narrowing limit ($\tau_c \ll \omega_0^{-1}$), in agreement with conclusions from our ^{2}H NMR lineshape analysis. For a 3-site 120° jump motion for reorientation of the $-ND_3$ group, and with the approximation $\eta = 0$, the powder average ^{2}H NMR spin–lattice relaxation time is given [23] (assuming that any contributions to spin–lattice relaxation from dipolar coupling to ^{14}N and ^{1}H are negligible) by

$$\langle 1/T_1 \rangle_p = \frac{9\pi^2}{40}\chi^2(\sin^4\beta + \sin^2 2\beta) \times \left(\frac{\tau_c}{1 + w_0^2\tau_c^2} + \frac{4\tau_c}{1 + 4w_0^2\tau_c^2}\right). \quad (2)$$

For $\tau_c \ll \omega_0^{-1}$, Eq. (2) can be simplified to

$$\langle 1/T_1 \rangle_p = \frac{9\pi^2}{2}\chi^2(\sin^4\beta + \sin^2 2\beta)\tau_c. \quad (3)$$

On the assumption of Arrhenius behavior for the temperature dependence of the correlation time [i.e., $\tau_c = \tau_c^0 \exp(E_a/RT)$, where τ_c^0 is the pre-exponential factor and E_a is the activation energy], Eq. (3) can be rearranged to give

$$\ln(\langle 1/T_1 \rangle_p^{-1}) = \ln\left(\frac{2}{9\pi^2\chi^2(\sin^4\beta + \sin^2 2\beta)\tau_c^0}\right) - \frac{E_a}{RT}. \quad (4)$$

Using our data, a plot of $\ln(\langle 1/T_1 \rangle_p^{-1})$ versus T^{-1} (shown in Fig. 4) is indeed linear, as predicted by Eq. (4), and from the gradient of the best-fit straight line, the activation energy is determined to be $E_a = 9.3 \pm 0.3\,kJ\,mol^{-1}$.

Eq. (2) was also used for a non-linear fit of the data shown in Fig. 4, taking $\chi = 204\,kHz$ (determined from the ^{2}H NMR lineshape analysis) and $\beta = 70.5°$, giving a best-fit value for the activation energy of $E_a = 9.2 \pm 0.3\,kJ\,mol^{-1}$. The non-linear fit in Fig. 4

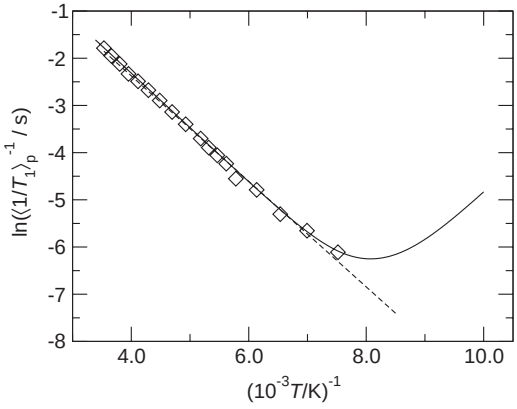

Fig. 4. ^{2}H NMR powder-average spin–lattice relaxation time of ATMA-d_3 plotted as $\ln[(\langle 1/T_1 \rangle_p)^{-1}/s]$ versus T^{-1}/K^{-1}.

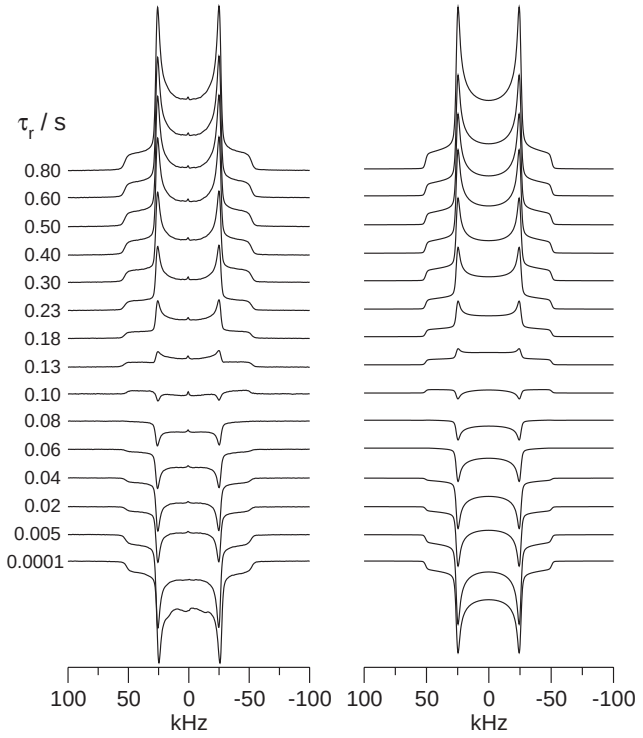

Fig. 5. Left—experimental ^{2}H NMR spectra of ATMA-d_3 recorded using the inversion-recovery technique as a function of the recovery time τ_r. Right—simulated ^{2}H NMR inversion-recovery spectra calculated using the 3-site 120° jump model discussed in the text and $\kappa = 3 \times 10^{10}\ s^{-1}$.

shows that, at 123 K (the lowest temperature accessible with the probe used in our work), $\langle 1/T_1 \rangle_p^{-1}$ is close to the minimum at which $\tau_c = 0.616\omega_0^{-1}$.

Partially relaxed inversion recovery ^{2}H NMR spectra of ATMA-d_3 were recorded at 298 K to characterize the anisotropy of the spin–lattice relaxation. The experimental results are shown in Fig. 5, together with simulated spectra calculated using the MXET1 program [24] for the 3-site 120° jump motion [with $\beta = 70.5°$ and taking the static quadrupole interaction parameters ($\chi = 204$ kHz and $\eta = 0$) obtained in our simulation of the experimental ^{2}H NMR lineshape at 298 K (see Section 3.1)]. Good agreement between the simulated and experimental partially relaxed lineshapes was achieved using $\kappa = 3 \times 10^{10}\ s^{-1}$.

To compare the simulated and experimental partially relaxed lineshapes, the anisotropy ΔR_1 of the spin–lattice relaxation was measured for both the experimental and simulated lineshapes using the equation [24]

$$\Delta R_1 = \frac{R_1(0°) - R_1(90°)}{R_1(0°) + R_1(90°)}, \quad (5)$$

where $R_1(\theta) = 1/T_1(\theta)$ and θ is the angle between the principal component of the (motionally averaged) electric field gradient tensor $\bar{V}_{ZZ}$ and the applied magnetic field B_0. The angle $\theta = 90°$ corresponds to the "horns" in the spectrum and $\theta = 0°$ corresponds to the outer edges ("wings") of the spectrum. $R_1(0°)$ and $R_1(90°)$ were determined by fitting the recovery curves for the intensities of the "wings" and the "horns" in the experimental and simulated spectra, giving $\Delta R_1 = +0.20$ for the experimental spectra and $\Delta R_1 = +0.19$ for the simulated spectra. The positive anisotropy reflects the fact that the relaxation is faster for the wings than the horns. The close agreement between the spin–lattice relaxation anisotropies for the experimental and simulated data further supports the 3-site 120° jump model for reorientation of the $-ND_3$ group. In particular, it was not necessary to resort to more complicated dynamic models involving small step diffusion within a three-fold potential for which, with low activation energies, the spin–lattice relaxation would be less anisotropic (i.e., $|\Delta R_1| < 0.20$).

3.3. ^{27}Al NMR

The ^{27}Al NMR spectrum of ATMA-d_3 recorded at 298 K is shown in Fig. 6a. The spectrum consists of a broad powder pattern, characteristic of the central $|+1/2\rangle \leftrightarrow |-1/2\rangle$ transition (recall that ^{27}Al has $I = 5/2$) broadened by the second order quadrupole interaction, together with a relatively narrow central line. The origin of the relatively narrow central line is probably the same as that of the central line in the ^{2}H NMR spectrum (Section 3.1). In simulations of the broad powder pattern, a reasonable fit to the

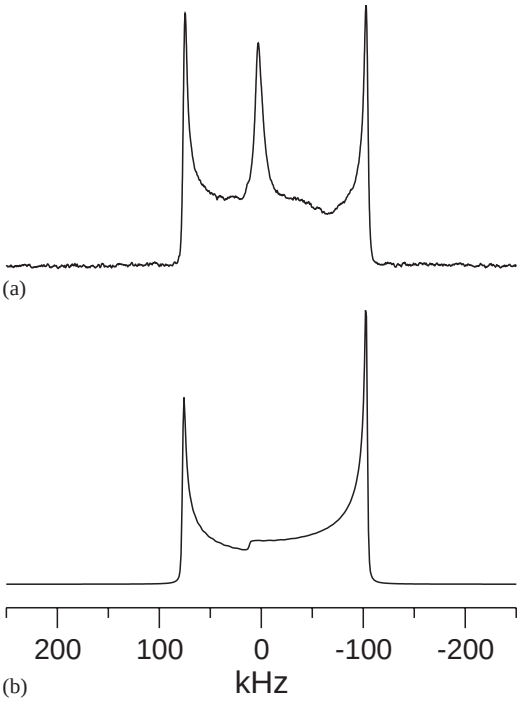

Fig. 6. (a) ^{27}Al NMR spectrum for a non-spinning sample of ATMA-d_3 recorded at 298 K using the spin-echo pulse sequence with $\tau = 50\ \mu s$. (b) Simulation of the ^{27}Al NMR spectrum of ATMA-d_3 with $\chi^{Al} = 21.25$ MHz and $\eta^{Al} = 0$.

experimental spectrum was achieved (Fig. 6b) using a quadrupole coupling constant χ^{Al} of 21.25 MHz and a quadrupole asymmetry parameter η^{Al} of 0.0 (note that chemical shift anisotropy and asymmetry were not included in the simulation). We note that, although the Al–N bond of the ATMA molecule in the crystal structure does not lie on a crystallographic three-fold rotation axis, the actual geometry of the molecule is nevertheless very close to C_3 symmetry, and a value of $\eta^{Al} \approx 0$ is therefore reasonable. These values of χ^{Al} and η^{Al} confirm that there is no exchange of the ND_3 and CH_3 groups of ATMA-d_3 (at least at a rate of $10^5\,s^{-1}$ or higher) which would give rise to tetrahedral averaging of the quadrupolar interaction tensor.

4. Concluding remarks

The ^2H NMR study of ATMA-d_3 reported here demonstrates clearly that, at all temperatures investigated (123–298 K), the $-ND_3$ group reorients rapidly by a 3-site 120° jump motion about the Al–N bond, with an activation energy of $9.3 \pm 0.3\,kJ\,mol^{-1}$. This activation energy is significantly lower than those reported for $-ND_3$ groups in many other materials [37–42] in which the $-ND_3$ groups (in contrast to ATMA) are involved in intermolecular hydrogen bonding. From our ^2H NMR and ^{27}Al NMR experiments, there is no evidence that any other large amplitude molecular motion occurs in the temperature range 123–298 K. In particular, there is no evidence for exchange between the $-ND_3$ and $-CH_3$ groups, confirming deductions [20] from the reported crystal structure that the $-ND_3$ and $-CH_3$ groups are ordered, corresponding to linear arrays of molecules with their Al–N bonds parallel. Recalling that the ATMA molecule has a significant electric dipole parallel to the Al–N bond, the formation of such linear arrays of ATMA molecules may be justified on the basis of strong intermolecular electrostatic (dipole–dipole) interactions.

From the NMR experiments reported here, site-exchange of the three $-CH_3$ groups by means of reorientation about the Al–N axis cannot be ruled out. Our studies of the ^2H and ^{27}Al NMR lineshapes and relaxation times of $(CH_3)_3AlND_3$ reported in this paper are not influenced by this type of reorientation, and ^2H NMR measurements on $(CD_3)_3AlNH_3$ would be the preferred technique for investigating the possible occurrence of this reorientational process. We note that this motion would not alter the orientation of the molecular dipole.

Acknowledgments

We are grateful to EPSRC and HEFCE for general support and to Glaxo Smith Kline for the award of a Ph.D. studentship (to GT).

References

[1] J.N. Sherwood (Ed.), The Plastically Crystalline State, Wiley, Chichester, 1979.
[2] G.N. Parsonage, L.A.K. Staveley, Disorder in Crystals, Oxford University Press, Oxford, 1978.
[3] J.D. Barnes, J. Chem. Phys. 58 (1973) 5193.
[4] M. Stohrer, F. Noack, J. Chem. Phys. 67 (1977) 3729.
[5] M.G. Taylor, E.C. Kelusky, I.C.P. Smith, H.L. Casal, D.G. Cameron, J. Chem. Phys. 78 (1983) 5108.
[6] F. Guillaume, J. Doucet, C. Sourisseau, A.J. Dianoux, J. Chem. Phys. 91 (1989) 2555.
[7] R. Tycko, G. Dabbagh, R.M. Fleming, R.C. Haddon, A.V. Makhija, S.M. Zahurak, Phys. Rev. Lett. 67 (1991) 1886.
[8] R.D. Johnson, C.S. Yannoni, H.C. Dorn, J.R. Salem, D.S. Bethune, Science 255 (1992) 1235.
[9] P. Launois, S. Ravy, R. Moret, Int. J. Mod. Phys. B 13 (1999) 253.
[10] D.W. McCall, D.C. Douglass, J. Chem. Phys. 33 (1960) 777.
[11] N.-I. Liu, J. Jonas, Chem. Phys. Lett. 14 (1972) 555.
[12] E.O. Stejskal, D.E. Woessner, T.C. Farrar, H.S. Gutowsky, J. Chem. Phys. 31 (1959) 55.
[13] S.B.W. Roeder, D.C. Douglass, J. Chem. Phys. 52 (1970) 5525.
[14] S. Takeda, G. Soda, H. Chihara, Mol. Phys. 47 (1982) 501.
[15] S. Albert, J.A. Ripmeester, J. Chem. Phys. 57 (1972) 2641.
[16] T. Hasebe, N. Nakamura, H. Chihara, Bull. Chem. Soc. Jpn. 61 (1988) 1803.
[17] A.E. Aliev, K.D.M. Harris, D.C. Apperley, J. Chem. Soc. Chem. Commun. (1993) 251.
[18] M.J. Jones, F. Guillaume, K.D.M. Harris, A.J. Dianoux, Proc. R. Soc. A 452 (1996) 701.
[19] A.E. Aliev, K.D.M. Harris, D.C. Apperley, R.K. Harris, J. Solid State Chem. 110 (1994) 314.
[20] J. Müller, U. Ruschewitz, O. Indris, H. Hartwig, W. Stahl, J. Am. Chem. Soc. 121 (1999) 4647.
[21] J. Seelig, Quart. Rev. Biophys. 10 (1977) 353.
[22] L.W. Jelinski, Ann. Rev. Mater. Sci. 15 (1985) 359.
[23] T.M. Alam, G.P. Drobny, Chem. Rev. 91 (1991) 1545.
[24] R.R. Vold, R.L. Vold, Adv. Magn. Opt. Reson. 16 (1991) 85.
[25] G.L. Hoatson, R.L. Vold, NMR Basic Principles and Progress, Vol. 32, Springer, Berlin, 1994, pp. 3–67.
[26] R.R. Vold, in: R. Tycko (Ed.), Nuclear Magnetic Resonance Probes of Molecular Dynamics, Kluwer Academic Publishers, Dordrecht, Hingham, MA, 1994, pp. 27–106.
[27] A.E. Aliev, E.J. MacLean, K.D.M. Harris, B.M. Kariuki, C. Glidewell, J. Phys. Chem. B 102 (1998) 2165.
[28] M. Bach-Vergés, S.J. Kitchin, K.D.M. Harris, M. Zugic, C.A. Koh, J. Phys. Chem. B 105 (2001) 2699.
[29] T.T. Ang, B.A. Dunnell, Can. J. Chem. 54 (1976) 1087.
[30] E.C. Reynhardt, J. Phys. C: Solid State Phys. 19 (1986) 1823.
[31] J. Müller, J. Am. Chem. Soc. 118 (1996) 6370.
[32] F.C. Sauls, L.V. Interrante, Z. Jiang, Z. Inorg. Chem. 29 (1990) 2989.
[33] D.P. Raleigh, R.G. Griffin, E.T. Olejniczak, J. Magn. Reson. 74 (1987) 464.
[34] M.S. Greenfield, A.D. Ronemus, R.L. Vold, R.R. Vold, P.D. Ellis, T.R. Raidy, J. Magn. Reson. 72 (1987) 89.
[35] J.H. Baltisberger, A. Pines, Computer Program CQP, University of California, Berkeley.
[36] P.O. Westlund, J. Magn. Reson. 145 (2000) 364.
[37] M.A. Keniry, R.L. Smith, H.S. Gutowsky, E. Oldfield, in: E. Clementi, R.H. Sarma (Eds.), Structure and Dynamics: Nucleic Acids and Proteins, Adenine Press, New York, 1983.
[38] J.R. Long, B.Q. Sun, A. Bowen, R.G. Griffin, J. Am. Chem. Soc. 116 (1994) 11950.

[39] M.A.K. Williams, R.D. Keenan, T.K. Halstead, Solid State NMR 6 (1996) 47.
[40] Z. Gu, K. Ebisawa, A. McDermott, Solid State NMR 7 (1996) 161.
[41] J.H. Kristensen, G.L. Hoatson, R.L. Vold, J. Chem. Phys. 110 (1999) 4533.
[42] S.J. Kitchin, S. Ahn, K.D.M. Harris, J. Phys. Chem. A 106 (2002) 7228.